nature communications

Article

https://doi.org/10.1038/s41467-026-68598-8

Ligand-controlled regiodivergent and enantioselective C–H cyanation of secondary amines

Received: 17 April 2025

Accepted: 12 January 2026

Published online: 20 January 2026

Check for updates

Yang-Jie Mao[1,2], Xiahe Chen[1,2], Huan-Le Li[1], Qi Pan[1], Kun Zhou[1], Zhen-Yuan Xu[1], Yun-Fang Yang[1] ✉, Shao-Jie Lou[1] ✉ & Dan-Qian Xu[1] ✉

Aliphatic amines, such as *N*,*N*-dialkyl secondary amines, represent important scaffolds in bioactive molecules, driving significant interest in their regio- and stereoselective C–H functionalisation. While hydrogen atom transfer (HAT) provides a powerful radical-based approach to elaborate such amines, achieving controllable, regio-divergent, and enantioselective functionalisation across different *N*-alkyl groups remains challenging. Herein, we report a Cu-catalyzed *α′*/*β*-regiodivergent and *β*-enantioselective cyanation of secondary amine-derived ureas through tunable 1,4′/1,5-HAT. The utilization of a sterically demanding ligand **L14** enables the excellent *α′*-selective C–H cyanation at the *N*-methyl position, while two developed ligands (**L24** and **L41**) promote the *β*-chirality construction at the other *N*-alkyl group. The approach is demonstrated for a broad scope of ureas with wide functional group compatibility. Experimental and computational studies reveal two distinct reaction pathways regarding the different reactive sites (*α′*/*β*) and the choice of ligands could significantly influence the selectivity in HAT process.

With an estimate of more than 60% of the top 200 small molecule pharmaceuticals by retail sales containing amine groups based on Njarðarson's reports, which are often along with chiral centers, there is an increasing need to devise streamlined and efficient synthetic methods to access these motifs[1,2]. In this context, developing a modular synthetic strategy that enables the site-divergent and enantioselective functionalisation of C(sp^3)–H bonds at different positions (*α*, *β*, *γ*, etc.) would be promising for the structural diversification of amines[3–6]. However, two or more different alkyl substituents on the amines makes the situation over double complicated compared to other compounds, albeit *α*-C–H bonds of amines might have higher reactivity for the appropriate bond dissociation energies (BDEs)[7–9]. By contrast to the *α*-site, reports concerning *β*-C–H bonds activation are rather less[10–14], and of course the *α*/*β* regio-divergent functionalisation of acyclic amines are still largely unexplored[15–17]. In addition, current methods for asymmetric *β*-C(sp^3)–H bond functionalisation of amines mainly focused on the intramolecular cycloamination[18–20] and the functionalisation of more reactive cyclic amines[11,16,21,22], while the enantioselective intermolecular C–H functionalisation at *β*-position of acyclic amines has met with limited success.

C(sp^3)–H bond functionalisation of amines through intramolecular hydrogen atom transfer (HAT) process, known as Hofmann-Löffler-Freytag (HLF) reaction, has become a powerful tool to assemble elaborated amines[23–25]. Generally, the H-abstraction triggered by nitrogen-centered radical (NCR) usually occurs at the *δ* position via intramolecular 1,5-HAT from N(1) to C(5), given the stability of six-membered, chair-like conformational transition state[26–29]. Nevertheless, incorporation of auxiliary groups (e.g., urea or sulfonylurea) can alter the reaction sites to *β*/*γ*-positions, which as well undergo the preponderant 1,5/6-HAT (Fig. 1A(a))[18,30–32]. In these cases, the regioselectivity is dominated by intramolecular HAT step and is highly relied on the structure of substrate, rather than the reaction conditions[20,33,34].

[1]Catalytic Hydrogenation Research Center, State Key Laboratory of Green Chemical Synthesis and Conversion, Key Laboratory of Green Pesticides and Cleaner Production Technology of Zhejiang Province, Zhejiang University of Technology, Hangzhou, Zhejiang, PR China. [2]These authors contributed equally: Yang-Jie Mao, Xiahe Chen. ✉e-mail: yangyf@zjut.edu.cn; loushaojie@zjut.edu.cn; chrc@zjut.edu.cn

https://doi.org/10.1038/s41467-026-68598-8

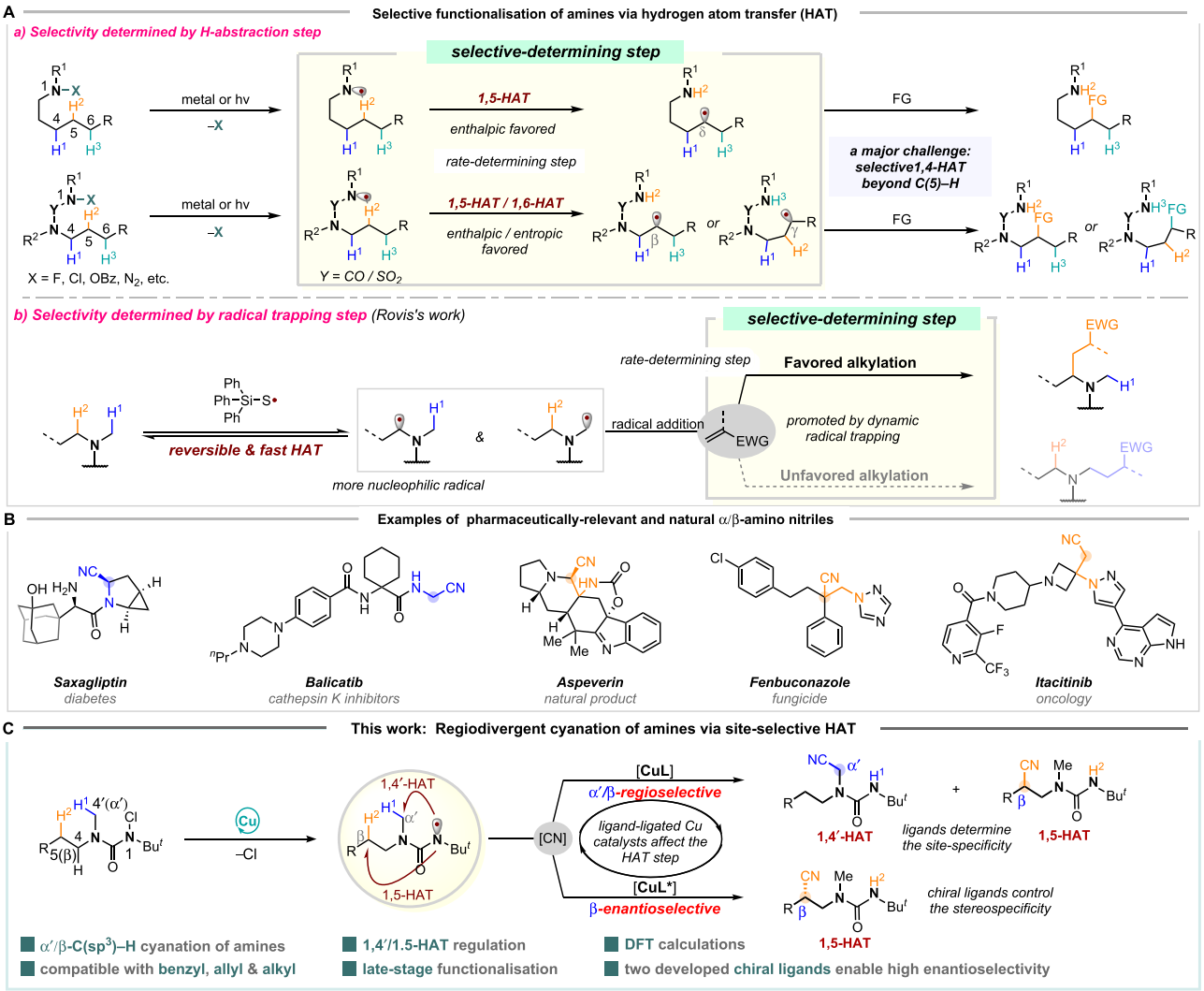

Fig. 1 | Site-selective *α′/β*-amino C(sp^3)–H bonds functionalisation. A Site-selective functionalisation of aliphatic amines through radical pathways; **B** Ubiquitous *α/β*-nitrile amine structural motifs in pharmaceuticals and natural product; **C** This work: regiodivergent and enantioselective cyanation of ureas through ligand-regulated selective hydrogen atom transfer of *α′/β*-amino C(sp^3)–H bonds.

Therefore, the radical transfer from *N* to other *C*-centered sites is of particularly difficult, especially for the rigid 1,4-HAT with coexisting of C(5) hydrogen[35]. Searching for suitable strategies that overcoming the intrinsic 1,5-HAT process is the key to unlock the *α/β* regio-divergent functionalisation of acyclic secondary amines.

Several elegant strategies have been developed for the site- and enantioselective C(sp^3)–H functionalisation of molecules possessing multiple similar C–H bonds[36–38]. For instance, Rovis and co-workers reported the site-selective C(sp^3)–H alkylation of tertiary amines at the more-crowded secondary *α*-position by turning the rate-determining step from hydrogen abstraction to radical trapping in the presence of a robust silylthiyl HAT catalyst (Fig. 1A(b))[38]. Alternatively, the groups of Liu and Lin also revealed that the Cu(II)-bound *N*-centered radical intermediates with a modular sulfonamide moiety and a specific bidentate ligand could be utilized as a tunable HAT reagent to discriminate the similar allylic C–H bonds in the same molecules[39,40]. Inspired by these precedents, we envisioned that the regiodivergent intramolecular HAT of secondary amines at different *N*-alkyl chains by NCRs could also be implemented by fine-tuning the ligand environment of the metal center.

On the other hand, the radical-mediated C–H cyanation has received great attention in recent years[34,40–46]. Given the importance of nitrile amines in medicine chemistry, the incorporation of a cyano-group onto amines at the different positions in a selective fashion is highly attractive in the discovery of drug molecules (Fig. 1B)[47,48]. Herein, we describe the ligand-controlled copper catalyzed regiodivergent and *β*-enantioselective cyanation of *N*-alkyl-*N*-methylamine-derived ureas by sliding 1,4′/1,5-HAT (Fig. 1C). Specifically, the more crowed ligand enabled the unusual 1,4′-HAT pathway to deliver *α*-amino radicals followed by kinetically favorable *N*-methyl cyanation while the sterically less demanding ligands promoted the *β*-cyanation through an entropically and enthalpically favored 1,5-HAT[34,49,50]. Moreover, the enantioselective *β*-cyanation was also achieved with two developed chiral ligands. The reaction features high regioselectivity and *β*-enantioselectivity, constituting an efficient pathway to access divergent cyano-substituted amines from the same set of starting materials. In addition, the mechanistic details have been elucidated by deuterium-labeling experiments and density functional theory (DFT) calculations.

Results

Reaction optimization

Current methods for asymmetric C(sp^3)–H bond functionalisation of amines via HLF process mainly relies on the initial generation of

https://doi.org/10.1038/s41467-026-68598-8

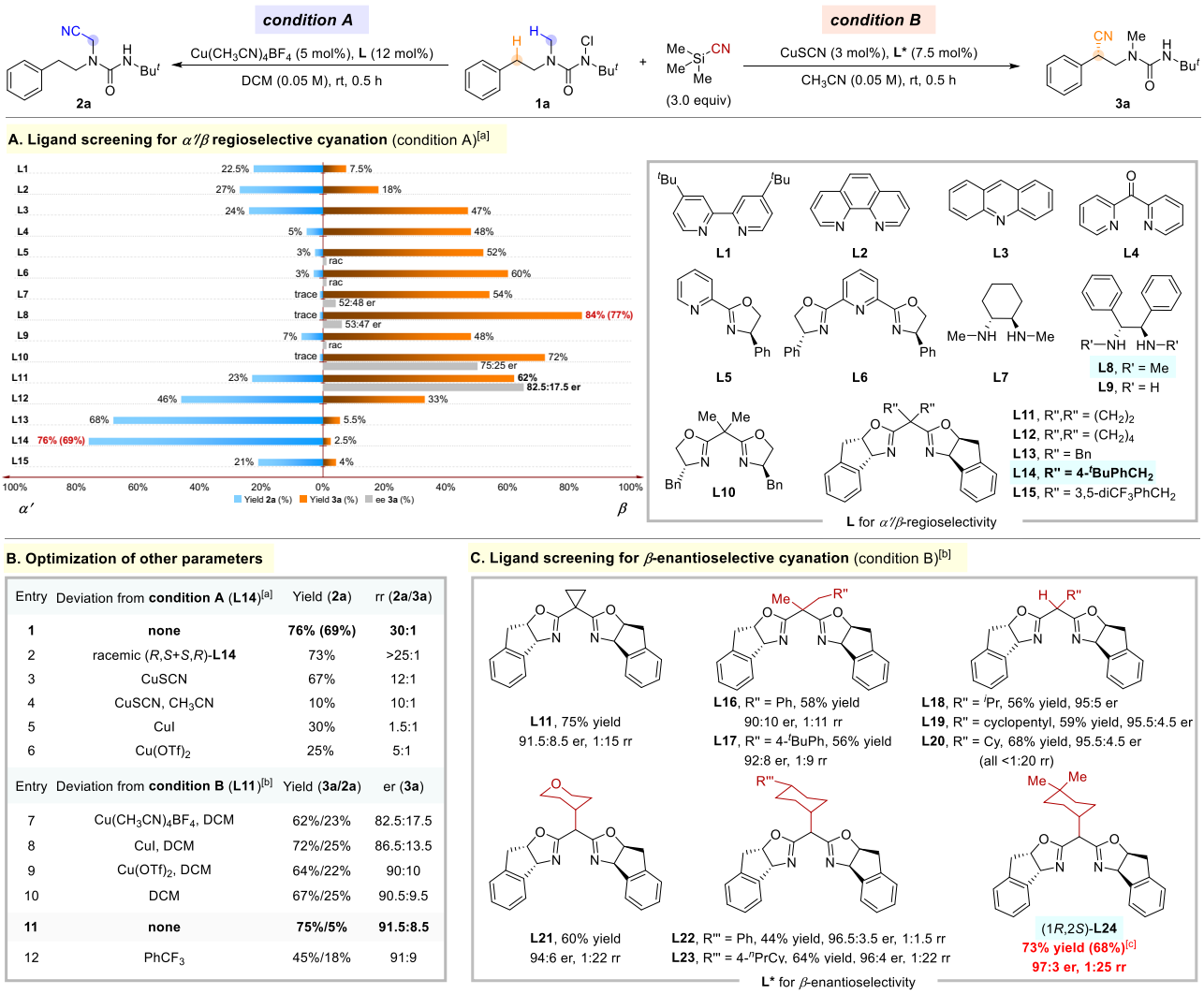

Entry	Deviation from **condition A** (**L14**)[a]	Yield (**2a**)	rr (**2a**/**3a**)
1	**none**	**76% (69%)**	**30:1**
2	racemic (*R*,*S*+*S*,*R*)-**L14**	73%	>25:1
3	CuSCN	67%	12:1
4	CuSCN, CH_3CN	10%	10:1
5	CuI	30%	1.5:1
6	$Cu(OTf)_2$	25%	5:1
Entry	Deviation from **condition B** (**L11**)[b]	Yield (**3a**/**2a**)	er (**3a**)
7	$Cu(CH_3CN)_4BF_4$, DCM	62%/23%	82.5:17.5
8	CuI, DCM	72%/25%	86.5:13.5
9	$Cu(OTf)_2$, DCM	64%/22%	90:10
10	DCM	67%/25%	90.5:9.5
11	**none**	**75%/5%**	**91.5:8.5**
12	$PhCF_3$	45%/18%	91:9

Fig. 2 | Optimization of reaction conditions. [a]Condition A: **1a** (26.9 mg, 0.1 mmol), TMSCN (29.7 mg, 0.3 mmol), $Cu(CH_3CN)_4BF_4$ (1.6 mg, 5 mol%), **L** (12 mol %), DCM (2 mL), N_2, rt, 0.5 h; [b]Condition B: **1a** (26.9 mg, 0.1 mmol), TMSCN (29.7 mg, 0.3 mmol), CuSCN (0.36 mg, 3 mol%), **L*** (7.5 mol%), CH_3CN (2 mL), N_2, rt, 0.5 h; [c]Isolation yield is in parentheses. The yields and regioselectivity ratios (rr, **2a**/**3a**) were determined by GC-MS using dodecane as internal standard, and the enantiomeric ratios (er) were determined by HPLC analysis. **A** Ligand screening for α′/β-regioselective cyanation; **B** Optimization of other parameters for α′-regioselective and β-enantioselective cyanation; **C** Ligand screening for β-enantioselective cyanation.

NCRs through homolytic cleavage of *N*-F[34,45,51–54] or *N*-O[55] precursors in the presence of transition metal catalysts or photoinduced catalysis. However, the analogous process triggered by homolytic cleavage of the readily-accessible *N*-Cl compounds have rarely been harnessed in these transformations, probably due to the fact that easy trapping of in-situ generated *C*-centered radicals by another *N*-Cl amine would usually lead to the side chlorination reaction or a subsequent intramolecular amination[32,33,56,57]. However, it has also been reported that the HLF process could be intercepted through the radical trapping by a Cu(II) intermediate and thereby results in the selective C(sp^3)–H bond functionalisation[58]. Given the well explored Cu-catalyzed radical-mediated C–H bond cyanation, we envisioned that chloroamide could be employed as a directing group for the regioselective C–H bond cyanation of amines via intercepted HLF process in the presence of copper/chiral bisoxazoline ligands catalytic systems[42,43,46,59]. With this consideration in mind, we commenced our investigation by firstly testing the $Cu(CH_3CN)_4BF_4$ catalysed α′/β-regioselective C–H bond cyanation of a *N*-Cl urea derivative of *N*-Me phenylethylamine (**1a**) with TMSCN in the presence of different *N*-containing ligands (Fig. 2A). The pyridine derived achiral ligands usually provided poor regioselectivity and only the utilization of di(2-pyridyl) ketone (**L4**) afforded the β-cyanation product **3a** with good regioselectivity (α′/β = 1:9). The chiral BOX and diamine ligands usually offered satisfactory β-siteselectivity, albeit with poor β-enantioselectivity (**L5**–**L10**). Among them, diamine ligand **L8** performed best, affording β-cyanation product **3a** in 77% isolated yield with excellent selectivity. Intriguingly, the use of ligand **L11** gave a mixture of **3a** and **2a** (62%/23% yield, respectively), and a promising enantioselectivity of **3a** was obtained (82.5:17.5 er). This result encouraged us to attempt a broader set of such ligands based on **L11**. To our surprise, the sterically more demanding analogous BOX ligands could give higher α′-selectivity and the ligand **L14** bearing bulky bis-4-^{t}BuBn group afforded the desired *N*-methyl cyanation product **2a** in 69% isolated yield with excellent 30:1 site-selectivity. Subjecting **1a** with racemic ligand (obtained by mixing (1*R*,2*S*)-**L14** and (1*S*,2*R*)-**L14**) gave a comparative yield and selectivity (Fig. 2B, entry 2). Further screening on various copper catalysts did not give better results for the selective formation of **3a** (Fig. 2B, entries 3–6). Next, we tried to enhance both the regio- and enantioselectivity for the β-cyanation of **3a** using **L11** as the ligand. After extensive evaluation of various reaction parameters (Fig. 2B, entries 7–12), CuSCN was identified as the optimal catalyst

https://doi.org/10.1038/s41467-026-68598-8

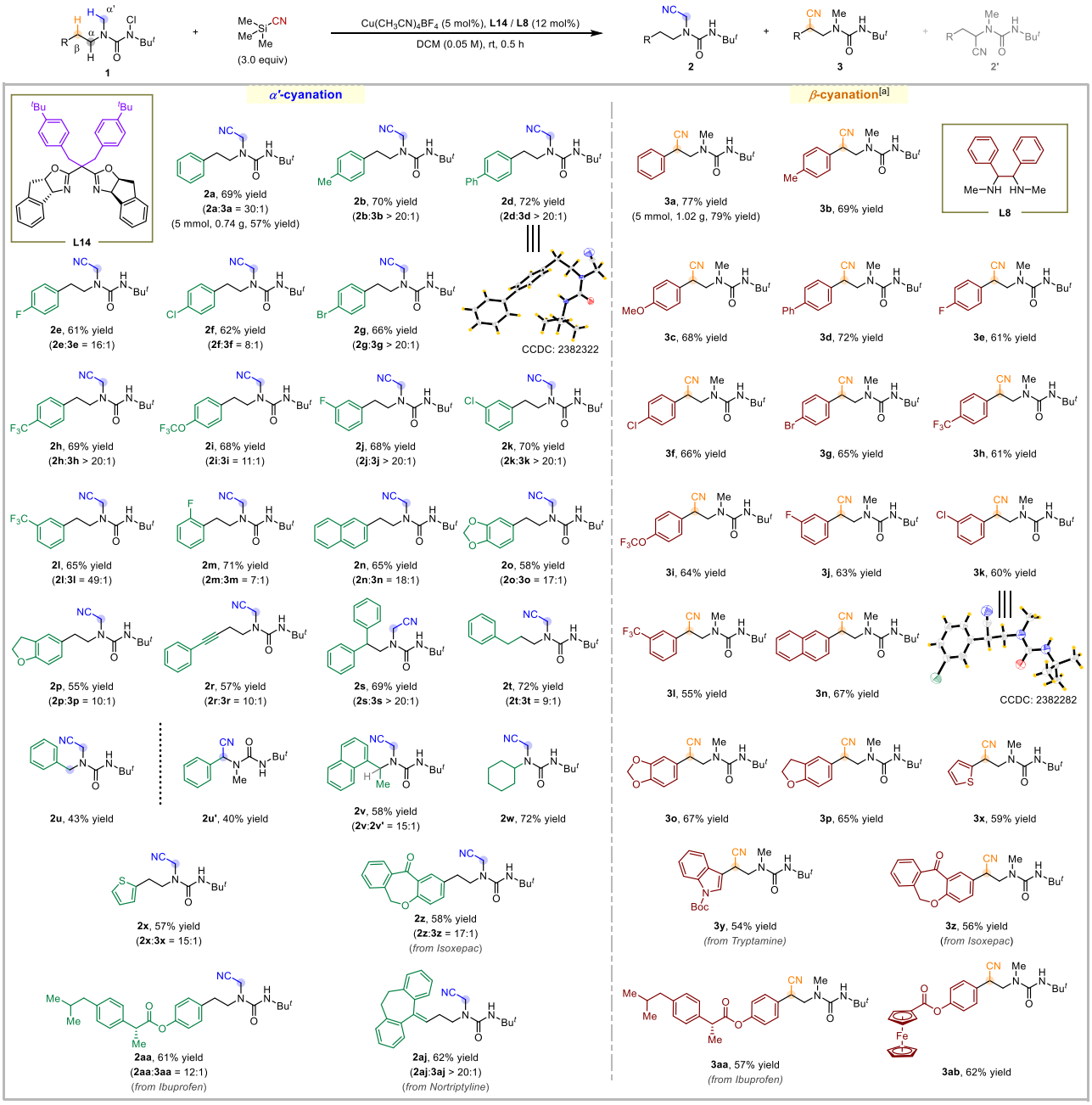

Fig. 3 | Scope of α'/β-cyanation. Condition A: **1** (0.2 mmol), $Cu(CH_3CN)_4BF_4$ (3.1 mg, 5 mol%), **L** (12 mol%), TMSCN (59.5 mg, 0.6 mmol), DCM (4 mL), N_2, rt, 0.5 h; isolated yield; the regioselectivity ratios (rr) were determined by GC-MS or HPLC. [a]All rr (**2**/**3**) < 1:20.

and CH_3CN was selected as the solvent, **3a** was obtained in good β-selectivity and enantioselectivity (75:5 rr and 91.5:8.5 er, entry 11). To further improve the enantio- and regioselectivity, a careful investigation of diverse chiral ligands under condition B was performed (Fig. 2C). It was found that the alkyl substituents at the central methylene position of BOX ligands could significantly influence the regio- and enantioselectivity probably through the modulation of bidentate bite angles[34]. For instance, the utilization of mono-alkyl (e.g., ^{i}Pr, cyclopentyl, cyclohexyl) substituted BOX ligands promoted the enantioselectivity to around 95:5 er (**L18**–**L20**). On the basis of these results, several designed BOX ligands bearing substituted cyclohexyl groups were prepared and tested (**L21**–**L24**). **L24** that possessing a 4,4-dimethylcyclohexyl group at the methylene position was identified as the optimized ligand, which afforded **3a** with both excellent enantioselectivity (97:3 er) and site-selectivity (25:1 β-selectivity).

Substrate scope

With the optimized reaction conditions in hand, the generality of developed strategy for the synthesis of α/β-nitrile amines was firstly investigated. Of note, despite various methods have been developed for α-C(sp^3)–H cyanation of secondary and tertiary amines, the regioselectivity among two or three side chains possibly cannot be circumvented given the co-existing of similar α-C–H bonds[60–65]. To our delight, the α-cyanation took place selectively at the *N*-methyl position of diverse urea protected *N*-methyl amines under the optimized condition A, as shown in Fig. 3, left. A variety of *N*-methyl phenylethylamine derivatives involving electronically diverse

substituents (e.g., Me, Ph, halo, CF_3 et al.) at *para*, *meta*, and *ortho* positions of the aromatic ring were readily accommodated to the reaction, affording the corresponding α-nitrile amines in good yields and α′-selectivity (**2a** and **2b, 2d**–**2m**). A larger gram-scale transformation of **1a** (5 mmol) also took place smoothly to afford the product **2a** in 57% yield. In the case of β-naphthylethylamine substrate, the product **2n** was obtained in 65% yield with 18:1 rr (α′/β). For disubstituted phenylethylamines, the reaction also proceeded well with moderate yield and decent site-selectivity (**2o** and **2p**). Besides the aryl group, the β-alkynyl substituent was also tolerated well in this C–C coupling process, delivering the desired products in moderate yield and good α′-selectivity (**2r**). Substrate bearing two phenyl groups at the β-position was compatible for α′-cyanation, despite the significant stability of possible β-benzylic radical (**2s**). Moreover, linear γ-phenylpropamine also survived the reaction condition, albeit with slightly decreased α′-selectivity (9:1), indicating that the **L14**-ligated Cu(II) intermediate could differentiate the subtle difference in steric environments of primary and common secondary C–H bonds (**2t**). In the case of *N*-Me benzylamine substrate that containing a competing highly reactive benzylic α-C–H bond, the α′-cyanation product **2u** could also be obtained by overriding the intrinsic reactivity en route **2u'** (rr = 1:1). Besides, the reaction of α-naphthylethylamine delivered product **2v** in a considerable yield with good selectivity at the primary α′-site over many other possible C–H bonds. Furthermore, functional groups such as, cyclohexyl (**2w**), and thienyl (**2x**) groups that tethered at the side chain of *N*-methyl amines were all tolerated without the loss in reaction efficiency or selectivity control. Notably, substrates that derived from pharmaceutical or bioactive molecules e.g., Isoxepac, Ibuprofen, and Nortriptyline could be well accommodated to the *N*-methyl C–H cyanation, allowing the valuable late-stage C–H functionalisation of complex molecules (**2z, 2aa** and **2aj**). Subsequently we explored the scope of β-cyanation of the same set of starting materials by simply changing the ligand **L14** to ligand **L8** (Fig. 3, right). Generally, the electron-donating and withdrawing substituents tethered at different positions of aromatic ring were all tolerated under the reaction conditions and had negligible influence on the reaction efficiency and regioselectivity (**3a** and **3b, 3c**–**3l**). The synthetic protocol for the β-cyanation also proved robust and readily scalable, with isolated 1.02 g of **3a** on a 5 mmol scale. Moreover, substrates bearing 2-naphthalene, 1,3-benzodioxole, 2,3-dihydrobenzofuran, and thienyl groups were compatible as well (**3n**–**3p, 3x**). The late-stage cyanation of structurally complex substrates containing bioactive moieties, such as Tryptamine, Isoxepac, and Ibuprofen, took place smoothly with exclusive β-selectivity (**3y**–**3aa**). Furthermore, the ferrocene group was also tolerated to the reaction, affording **3ab** in 62% yield. These results further demonstrate that the regio-divergency could be well regulated in the presence of different ligands.

In light of the lack of adaptive strategy for constructing β-chiral centers of amines via intermolecular C–H conversion[11], we next explored the applicability of these asymmetric β-cyanation protocol. Generally, a suite of *N*-Me phenylethylamines were site-specifically transformed into the optical pure β-nitrile amines with comparable yields, excellent regio- and enantioselectivity (Fig. 4). Both electron-donating (**3a***–**3d***) and electron-withdrawing (**3e***–**3i***) substituents at *para*-position were tolerated to the reaction with satisfactory results (er > 95:5 in most cases). To demonstrate the practical utility and scalability of this methodology, a large-scale (5 mmol) synthesis of the chiral compound **3a*** was carried out and a comparable result was obtained. Moreover, *meta*-substituted phenylethylamines were subjected to the reaction conditions and the corresponding cyanation products **3j***–**3l*** were formed with intact yields and selectivity. It is worth mentioning that substrate bearing *ortho*-F group delivered the product **3 m*** in 65% yield, along with excellent 99:1 er and over 20:1 β-selectivity. Moreover, the reaction also exhibited perfect compatibility with di-substituted substrates at both 3,4-positions of aromatic ring (**3n***–**3q***). Varying the phenyl derivatives to thiophene did not hamper the reactivity of the reaction, albeit with slightly decreased yield and selectivity (**3x***). Importantly, several complex bioactive relevant molecules were compatible as well and the corresponding chiral β-cyanation products were successfully obtained with excellent regio- and enantioselectivity (**3y***–**3aa***). Intriguingly, the protocol could also provide rapid access to both enantiomers by simply alternating the configuration of chiral ligand (**3z*** & ***ent*-3z***). In addition, this methodology also worked smoothly with ferrocene-containing substrate, which gave **3ab*** with excellent enantioselectivity and site-selectivity (95:5 er, 18:1 rr). The absolute configuration of **3a*** was determined to be *S* by comparing the optical rotation and the chiral HPLC diagram of a **3a*** derivative with that of an authentic chiral sample (See Section 6 in Supplementary Information for details). That of the other cyanation products was assigned accordingly.

Next, inspired by Liu's work on the asymmetric allylic C–H bond cyanation[40], we continued to investigate the asymmetric allylic β-C–H cyanation of amines under the developed condition B. However, a series of oxazoline-derived chiral ligands including **L24** gave negative results. Gratifyingly, after extensive exploration of diverse ligands, it was found that the elaborately modified chiral diamine ligand (1*S*,2*S*)-**L41**, which was designed by incorporating two particular bulky groups as "long spreading arms" at side chains[66], could provide decent enantioselectivity with exclusive β-selectivity (see Table S6 in Supplementary Information for more details). Under these conditions, various *N*-methyl homoallylic amines were efficiently converted into the stereochemically pure cyanides with comparable enantioselectivity (**3ac*** –**3af***). Furthermore, the cyanation of 1,1-disubstitutied olefins also took place smoothly and only the β-nitrile chiral amines were obtained with good enantioselectivity (**3ag***–**3aj***). Beyond aryl alkylene variants, cycloalkenes were also tested, furnishing the target products with excellent regioselectivity and acceptable enantioselectivity (**3ak*** and **3al***).

Mechanistic studies

To get further insight into the reaction mechanism, several control experiments and isotope labeling experiments were conducted. It was previously found that the reaction of **1u**, a substrate having both *N*-methyl and *N*-benzyl moieties, under the condition A led the formation of a mixture of **2u**/**2u'** (Fig. 3). However, running the reaction in the absence of **L14** exclusively provided the benzylic cyanation product **2u'** (Fig. 5A). It is in line with the fact that benzyl C–H bond is more likely to undergo intramolecular 1,4-HAT than methyl because of the stabilized benzylic radical[67]. These results also suggest that the ligand should play a pivotal role in regioselectivity control and could even reverse the intrinsic reactivity. To elucidate the different radical species involved in the selective cyanation mechanism, a series of radical experiments were conducted (Fig. 5B). The addition of radical inhibitor 2,2,6,6-tetramethyl-1-piperdinyloxy (TEMPO) to the standard conditions of either condition A or condition B completely shut down the reactions, suggesting that these two reactions should proceed through radical pathways (Fig. 5B(a)). However, the α′-radical adduct product **2a-BHT** was not observed in the presence of butylated hydroxytoluene (BHT) under condition A, probably due to the instability of primary methyl radical. In contrast, the formation of the β-radical was verified by the identification of its trapping product **3a-BHT** under condition B (Fig. 5B(b)). Overall, these results firmly establish the involvement of radical pathways in the selective cyanation mechanism. Moreover, the non-linear effect study of **1a** revealed a linear relationship between the ee value of **3a*** and ligand (1*R*,2*S*)-**L24**, implying that a single chiral ligand-ligated copper intermediate should be involved in the enantio-determining transition state (Fig. 5C). Next, a series of deuterium-labeling experiments were performed to probe the nature of C–H bond cleavage steps. The cyanation of deuterated substrate **1a-[*α′*]*d*$_3$**

https://doi.org/10.1038/s41467-026-68598-8

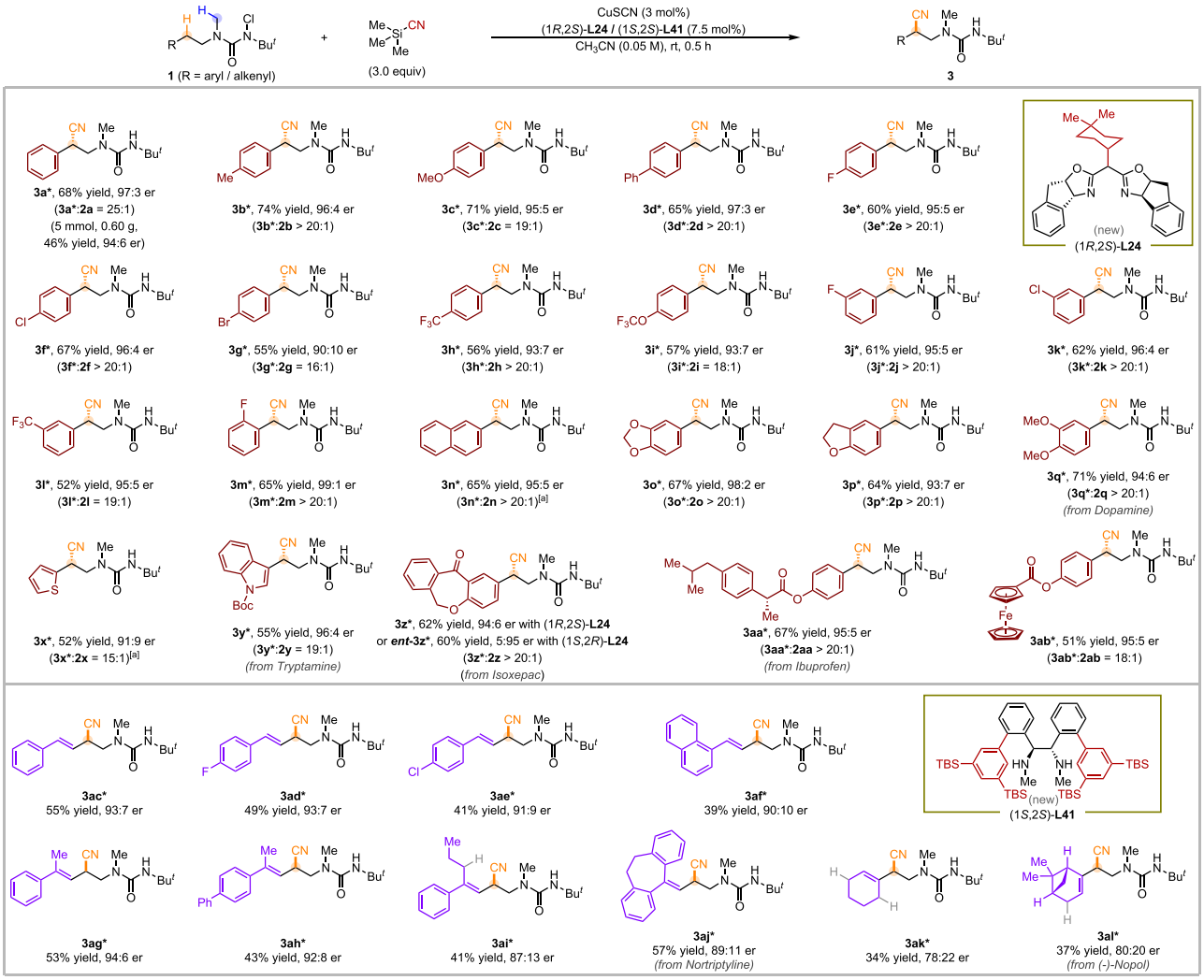

Fig. 4 | Scope of enantioselective *β*-cyanation. Condition B: **1** (0.2 mmol), CuSCN (0.7 mg, 3 mol%), **L*** (7.5 mol%), TMSCN (59.5 mg, 0.6 mmol), CH_3CN (4 mL), N_2, rt, 0.5 h; isolated yield; the regioselectivity ratios (rr) were determined by GC-MS analysis or HPLC, and the enantiomeric ratios (er) were determined by HPLC analysis. [a]$Cu(OTf)_2$ (3 mol%) was used.

under condition B provided the *β*-nitrile product **3a*-[*α′*]*d*$_3$** while the *N*-CD_3 remained intact (Fig. 5D(a)). In sharp contrast, treating **1a-[*α′*]*d*$_3$** with condition A resulted in the formation of a 1:1 mixture of **2a-[*α′*]*d*$_2$** and **3a*-[*α′*]*d*$_3$**, in which no H/D distribution between *α′* and *β* positions were observed (Fig. 5D(b)). These results unambiguously demonstrate that the site-divergent C−H cyanation undergoes straightforward 1,5-HAT or 1,4′-HAT, rather than reversible HAT process[36,38] or radical transfer process (e.g., *α′*-C radical to *β*-C radical through 1,4-HAT)[67,68]. Furthermore, the successful regioselectivity control partially relied on the similar BDE of *β*-benzylic and *α′* hydrogens (~89 kcal/mol vs ~93 kcal/mol)[7], since a poor regioselectivity (1:1) was obtained when increasing the BDE of *α′*-C−H bonds by replacing *N*-CH_3 with *N*-CD_3 (~89 kcal/mol vs ~96 kcal/mol, Fig. 5D(b)). Finally, several kinetic isotopic effect (KIE) experiments were conducted between different **1a-*d*$_n$** (*n* = 0, 2–5) in mixed and parallel modes. The obtained KIE values of *α′*-cyanation from intermolecular competition (KIE = 2.2) and parallel reactions (KIE = 2.1) under condition A suggested that the 1,4′-HAT process might be the rate-determining step (Fig. 5E). Moreover, large primary KIE values ($k_H/k_D > 2.5$) were observed either in the intermolecular/intramolecular *β*-H/D competing reaction, or two parallel reactions under condition B, indicating that the 1,5-HAT process is probably involved in the rate-determining steps in the presence of (1*R*,2*S*)-**L24** (Fig. 5F)[69].

To gain insight into the origin of selectivity, DFT calculations were performed (See Section 8 in Supplementary Information for details). The free energy profiles for C−H cyanation at the *β*- and *α′*-positions in the Cu(CN)(**L24**) system are shown in Figs. S16–S18[70,71]. DFT results indicate that the HAT step serves as the rate-determining step, consistent with the kinetic isotope effect experiments, whereas the enantioselectivity in *β*-C−H cyanation is established during the radical recombination and reductive elimination steps. The steric repulsion between the substrate and the **L24** ligand was found to play a crucial role in the observed enantioselectivity (Fig. S19). For the Cu(CN)(**L14**) system, the regioselectivity calculations were focused on the HAT step, which was identified as irreversible. The computed transition states show a small energetic preference for the pathway leading to the experimentally observed *α′*-cyanation product (Fig. S21). Additional analysis suggests that weak noncovalent interactions may contribute to stabilizing the transition state (Fig. S22).

Discussion

In this work, we have achieved the regio-divergent *α′*/*β*-C(sp^3)−H bonds cyanation of secondary *N*-alkyl-*N*-methyl amines through ligand-controlled selective 1,4′/1,5-HAT. The reaction indicated that the presence of bulky ligand could facilitated the *α′*-selective C−H cyanation of secondary amines at the *N*-methyl moiety, while the less

https://doi.org/10.1038/s41467-026-68598-8

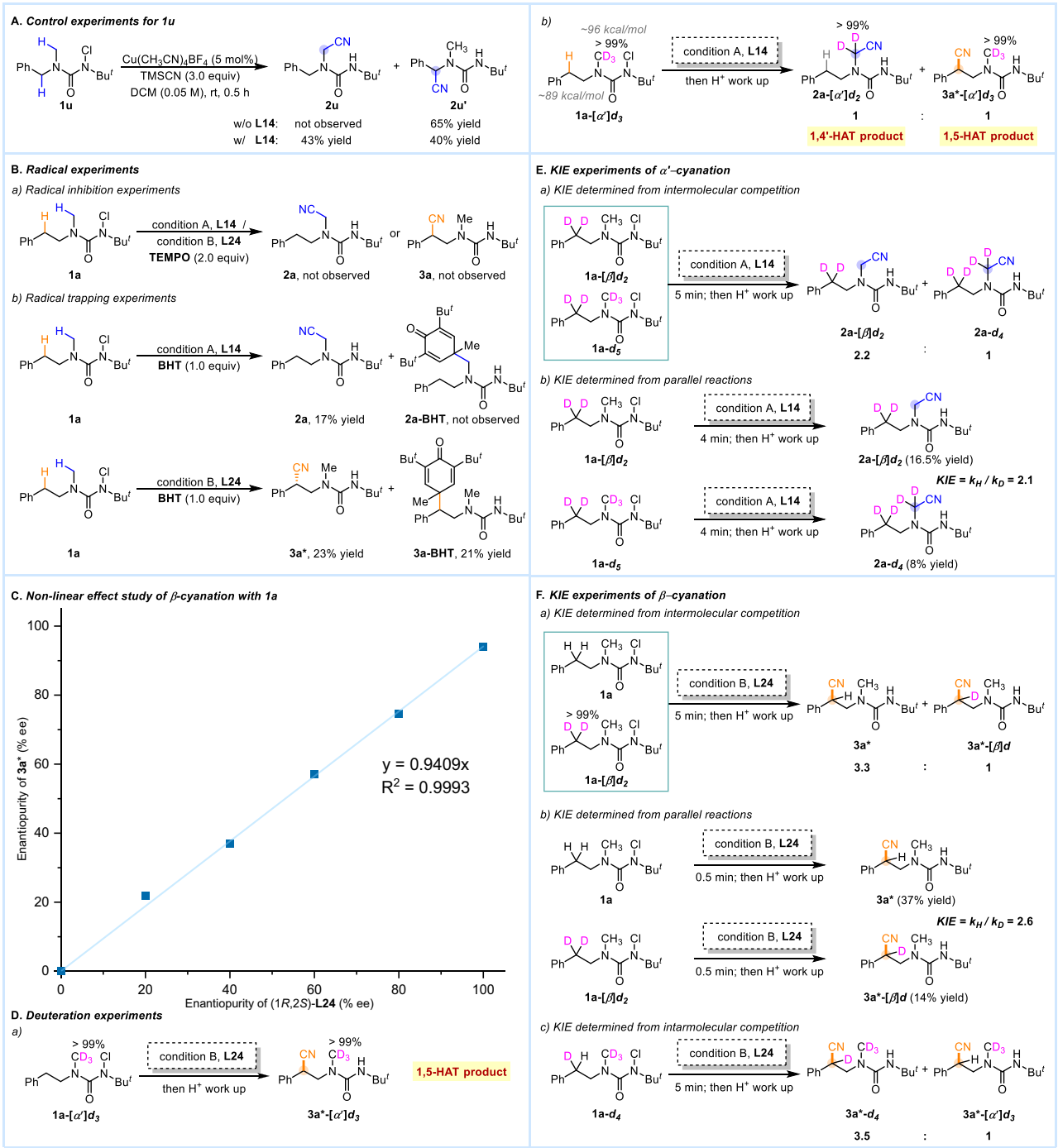

Fig. 5 | Control experiments and preliminary mechanistic study. Condition A: $Cu(CH_3CN)_4BF_4$ (5 mol%), **L14** (12 mol%), TMSCN (3.0 equiv), DCM (0.05 M), N_2, rt; Condition B: CuSCN (3 mol%), (1*R*,2*S*)-**L24** (7.5 mol%), TMSCN (3.0 equiv), CH_3CN (0.05 M), N_2, rt. More details see SI. **A** Control experiments for **1 u** with/without **L14**; **B** Radical inhibition and trapping experiments under condition A/B; **C** Non-linear effect study of *β*-cyanation under condition B; **D** Deuteration experiments; **E** KIE experiments of *α'*-cyanation under condition A; **F** KIE experiments of *β*-cyanation under condition B.

sterically demanding diamine ligand enabled the *β*-cyanation. Furthermore, two chiral ligands were developed that successfully mediated the enantioselective C−H cyanation of secondary amines at *β*-benzylic and allylic positions. This protocol facilitates rapid cyanation of various secondary amine-derived ureas under mild conditions, demonstrating broad substrate compatibility, excellent *α'*/*β*-regioselectivity, and remarkable *β*-enantioselectivity. Mechanistic studies suggest that the copper-bounded NCR species with different ligand environments plays a critical role in site selectivity during the irreversible HAT step, and the following two distinct reaction models would eventually lead to the regiodivergent C−H cyanation of secondary amines at different sites. In addition, the origin of the high site- and enantioselectivity has also been clarified by the DFT calculations. This study not only provides the alternative strategy for the regiodivergent and enantioselective C−H functionalisation of amines but also deepens the mechanistic understanding in the controllable HAT process. The pursue of ligand-controlled diverse functionalisation of dialkylamines with other reagents through selective HAT is on the way in our laboratory.

Methods

Regioselective for the α′/β-C(sp^3)–H cyanation (Condition A)

In a dried sealed 10 mL Schlenk tube equipped with a stir bar, $Cu(CH_3CN)_4BF_4$ (0.01 mmol, 5 mol%), **L14**/**L8** (0.024 mmol, 12 mol%) and *N*-chloro substrate **1** (0.2 mmol) were dissolved in degassed DCM (4 mL) under N_2 atmosphere, then TMSCN (0.6 mmol) was added. The tube was sealed with Teflon septum and stirred at room temperature for 0.5 h. After completed, the mixture was concentrated under reduced pressure, and the residue was purified by column chromatography or preparative thin-layer chromatography (PE/EA = 10/1) to provide desired products **2**/**3**.

Enantioselective for the β-C(sp^3)–H cyanation (Condition B)

In a dried sealed 10 mL Schlenk tube equipped with a stir bar, CuSCN (0.006 mmol, 3 mol%), (1*R*,2*S*)-**L24**/(1*S*,2*S*)-**L41** (0.015 mmol, 7.5 mol%) and *N*-chloro substrate **1** (0.2 mmol) were dissolved in degassed CH_3CN (4 mL) under N_2 atmosphere, then TMSCN (0.6 mmol) was added. The tube was sealed with Teflon septum and stirred at room temperature for 0.5 h. After completed, the mixture was concentrated under reduced pressure, and the residue was purified by column chromatography or preparative thin-layer chromatography (PE/EA = 10/1) to provide desired products **3***.

Data availability

The experimental data generated in this study are provided in the Supplementary Information. The computational coordinate data generated in this study are provided in the Source Data, The X-ray crystallographic coordinates for structures reported in this study have been deposited at the Cambridge Crystallographic Data Centre (CCDC), under deposition numbers of CCDC 2382322 (**2d**), and CCDC 2382282 (**3k**). These data can be obtained free of charge from The Cambridge Crystallographic Data Centre via www.ccdc.cam.ac.uk/data_request/cif. All data are available from the corresponding author upon request. Source data are provided with this paper.

References

1. Hu, S. et al. Ni-catalyzed enantioselective reductive cyclization/amidation and amination of 1,6-enynes and 1,7-enynes. *Angew. Chem. Int. Ed.* **63**, e202413892 (2024).
2. Flick, A. C. et al. Synthetic approaches to the new drugs approved during 2019. *J. Med. Chem.* **64**, 3604–3657 (2021).
3. Chen, L. et al. Photocatalytic carboxylation of C–N bonds in cyclic amines with CO_2 by consecutive visible-light-induced electron transfer. *Angew. Chem. Int. Ed.* **62**, e202217918 (2023).
4. Ni, S.-F. et al. Recent advances in γ-C(sp^3)–H bond activation of amides, aliphatic amines, sulfanilamides and amino acids. *Coord. Chem. Rev.* **455**, 214255 (2022).
5. Wu, X. & Zhu, C. Radical functionalization of remote C(sp^3)–H bonds mediated by unprotected alcohols and amides. *CCS Chem.* **2**, 813–828 (2020).
6. He, C., Whitehurst, W. G. & Gaunt, M. J. Palladium-catalyzed C(sp^3)–H bond functionalization of aliphatic amines. *Chem* **5**, 1031–1058 (2019).
7. Le, C., Liang, Y., Evans, R. W., Li, X. & MacMillan, D. W. C. Selective sp^3 C–H alkylation *via* polarity-match-based cross-coupling. *Nature* **547**, 79–83 (2017).
8. Loh, Y. Y. et al. Photoredox-catalyzed deuteration and tritiation of pharmaceutical compounds. *Science* **358**, 1182–1187 (2017).
9. Shaw, M. H., Shurtleff, V. W., Terrett, J. A., Cuthbertson, J. D. & MacMillan, D. W. C. Native functionality in triple catalytic cross-coupling: sp^3 C–H bonds as latent nucleophiles. *Science* **352**, 1304–1308 (2016).
10. Chen, J., Tan, C., Rodrigalvarez, J., Zhang, S. & Martin, R. Site-selective distal C(sp3)–H bromination of aliphatic amines as a gateway for forging nitrogen-containing sp^3 architectures. *Angew. Chem. Int. Ed.* **63**, e202406485 (2024).
11. Chang, Y. et al. Enantioselective synthesis of *N*-alkylamines through β-amino C–H functionalization promoted by cooperative actions of $B(C_6F_5)_3$ and a chiral lewis acid co-catalyst. *J. Am. Chem. Soc.* **143**, 2441–2455 (2021).
12. Sarver, P. J. et al. The merger of decatungstate and copper catalysis to enable aliphatic C(sp^3)–H trifluoromethylation. *Nat. Chem.* **12**, 459–467 (2020).
13. Huang, Z., Wang, C. & Dong, G. A hydrazone-based exo-directing-group strategy for β C–H oxidation of aliphatic amines. *Angew. Chem. Int. Ed.* **55**, 5299–5303 (2016).
14. McNally, A., Haffemayer, B., Collins, B. S. L. & Gaunt, M. J. Palladium-catalysed C–H activation of aliphatic amines to give strained nitrogen heterocycles. *Nature* **510**, 129–133 (2014).
15. Rumo, C. et al. An artificial metalloenzyme based on a copper heteroscorpionate enables sp^3 C–H functionalization *via* intramolecular carbene insertion. *J. Am. Chem. Soc.* **144**, 11676–11684 (2022).
16. Lin, W., Zhang, K.-F. & Baudoin, O. Regiodivergent enantioselective C–H functionalization of Boc-1,3-oxazinanes for the synthesis of β^2- and β^3-amino acids. *Nat. Catal.* **2**, 882–888 (2019).
17. Millet, A., Dailler, D., Larini, P. & Baudoin, O. Ligand-controlled α- and β-arylation of acyclic *N*-boc amines. *Angew. Chem., Int. Ed.* **53**, 2678–2682 (2014).
18. Zhou, Z. et al. Enantioselective ring-closing C–H amination of urea derivatives. *Chem* **6**, 2024–2034 (2020).
19. Lang, K., Torker, S., Wojtas, L. & Zhang, X. P. Asymmetric induction and enantiodivergence in catalytic radical C–H amination *via* enantiodifferentiative H-atom abstraction and stereoretentive radical substitution. *J. Am. Chem. Soc.* **141**, 12388–12396 (2019).
20. Yang, Y., Cho, I., Qi, X., Liu, P. & Arnold, F. H. An enzymatic platform for the asymmetric amination of primary, secondary and tertiary C(sp^3)–H bonds. *Nat. Chem.* **11**, 987–993 (2019).
21. Kuroda, Y. et al. An iridium/aluminum cooperative strategy for the β-C(sp^3)-H borylation of saturated cyclic amines. *Angew. Chem. Int. Ed.* **62**, e202300704 (2023).
22. Smalley, A. P., Cuthbertson, J. D. & Gaunt, M. J. Palladium-catalyzed enantioselective C–H activation of aliphatic amines using chiral anionic binol-phosphoric acid ligands. *J. Am. Chem. Soc.* **139**, 1412–1415 (2017).
23. Lv, X., Yang, Y., Zhou, L. & Zeng, X. Copper-catalyzed fluoroamide-directed remote C(sp^3)-H bond functionalization through intramolecular hydrogen atom transfer. *Eur. J. Org. Chem.* **27**, e202400027 (2024).
24. Zhang, Z., Chen, P. & Liu, G. Copper-catalyzed radical relay in C(sp^3)–H functionalization. *Chem. Soc. Rev.* **51**, 1640–1658 (2022).
25. Muñoz-Molina, J. M., Belderrain, T. R. & Pérez, P. J. Recent advances in copper-catalyzed radical C–H bond activation using *N*–F reagents. *Synthesis* **53**, 51–64 (2021).
26. Sinha, S. K. et al. Toolbox for distal C–H bond functionalizations in organic molecules. *Chem. Rev.* **122**, 5682–5841 (2022).
27. Sarkar, S., Cheung, K. P. S. & Gevorgyan, V. C–H functionalization reactions enabled by hydrogen atom transfer to carbon-centered radicals. *Chem. Sci.* **11**, 12974–12993 (2020).
28. Zhang, Z.-H., Wei, H., Li, Z.-L. & Liu, X.-Y. Recent advances in radical-involved alkynylation of unactivated C(sp^3)–H bonds by hydrogen atom abstraction. *Synlett* **32**, 362–369 (2020).
29. Stateman, L. M., Nakafuku, K. M. & Nagib, D. A. Remote C–H functionalization *via* selective hydrogen atom transfer. *Synthesis* **50**, 1569–1586 (2018).
30. Simons, R. T. et al. Directed photochemically mediated nickel-catalyzed (hetero)arylation of aliphatic C–H bonds. *J. Am. Chem. Soc.* **145**, 3882–3890 (2023).

31. Bafaluy, D., Georgieva, Z. & Muñiz, K. Iodine catalysis for C(sp^3)–H fluorination with a nucleophilic fluorine source. *Angew. Chem. Int. Ed.* **59**, 14241–14245 (2020).
32. Short, M. A., Shehata, M. F., Sanders, M. A. & Roizen, J. L. Sulfamides direct radical-mediated chlorination of aliphatic C–H bonds. *Chem. Sci.* **11**, 217–223 (2020).
33. Nanjo, T., Matsumoto, A., Oshita, T. & Takemoto, Y. Synthesis of chlorinated oligopeptides *via* γ- and δ-selective hydrogen atom transfer enabled by the *N*-chloropeptide strategy. *J. Am. Chem. Soc.* **145**, 19067–19075 (2023).
34. Zhang, Z., Zhang, X. & Nagib, D. A. Chiral piperidines from acyclic amines *via* enantioselective, radical-mediated δ C–H cyanation. *Chem* **5**, 3127–3134 (2019).
35. He, Y., Tian, C., An, G. & Li, G. β-C(sp3)–H chlorination of amide derivatives *via* photoinduced copper charge transfer catalysis. *Chin. Chem. Lett.* **35**, 108546 (2024).
36. Wang, M., Huang, Y. & Hu, P. Terminal C(sp3)–H borylation through intermolecular radical sampling. *Science* **383**, 537–544 (2024).
37. Xu, J. et al. Site-selective α-C(sp^3)–H arylation of dialkylamines *via* hydrogen atom transfer catalysis-enabled radical aryl migration. *Nat. Commun.* **15**, 6791 (2024).
38. Shen, Y., Funez-Ardoiz, I., Schoenebeck, F. & Rovis, T. Site-selective α-C–H functionalization of trialkylamines *via* reversible hydrogen atom transfer catalysis. *J. Am. Chem. Soc.* **143**, 18952–18959 (2021).
39. Li, J. et al. Mechanistic insights into copper-catalyzed asymmetric cyanation of allylic C–H bonds. *J. Am. Chem. Soc.* **147**, 14756–14768 (2025).
40. Li, J. et al. Site-specific allylic C–H bond functionalization with a copper-bound *N*-centred radical. *Nature* **574**, 516–521 (2019).
41. Chen, K. et al. Functional-group translocation of cyano groups by reversible C–H sampling. *Nature* **620**, 1007–1012 (2023).
42. Cai, C.-Y. et al. Photoelectrochemical asymmetric catalysis enables site- and enantioselective cyanation of benzylic C–H bonds. *Nat. Catal.* **5**, 943–951 (2022).
43. Wang, F., Chen, P. & Liu, G. Copper-catalysed asymmetric radical cyanation. *Nat. Synth.* **1**, 107–116 (2022).
44. Bao, X., Wang, Q. & Zhu, J. Dual photoredox/copper catalysis for the remote C(sp3)–H functionalization of alcohols and alkyl halides by *N*-alkoxypyridinium salts. *Angew. Chem. Int. Ed.* **58**, 2139–2143 (2019).
45. Wang, C.-Y. et al. Enantioselective copper-catalyzed cyanation of remote C(sp^3)-H bonds enabled by 1,5-hydrogen atom transfer. *iScience* **21**, 490–498 (2019).
46. Zhang, W. et al. Enantioselective cyanation of benzylic C–H bonds *via* copper-catalyzed radical relay. *Science* **353**, 1014–1018 (2016).
47. Qian, S., Lazarus, T. M. & Nicewicz, D. A. Enantioselective amino- and oxycyanation of alkenes *via* organic photoredox and copper catalysis. *J. Am. Chem. Soc.* **145**, 18247–18252 (2023).
48. Duan, S. et al. Catalytic chemo- and regioselective radical carbocyanation of 2-azadienes for the synthesis of α-amino nitriles. *Angew. Chem. Int. Ed.* **62**, e202300605 (2023).
49. Bower, J. K. et al. C(sp^3)–H cyanation by a formal copper(III) cyanide complex. *Chem. Sci.* **14**, 1301–1307 (2023).
50. Ratani, T. S., Bachman, S., Fu, G. C. & Peters, J. C. Photoinduced, copper-catalyzed carbon–carbon bond formation with alkyl electrophiles: cyanation of unactivated secondary alkyl chlorides at room temperature. *J. Am. Chem. Soc.* **137**, 13902–13907 (2015).
51. Wang, W. et al. Copper-catalyzed asymmetric remote C(sp^3)–H alkylation of *N*-fluorocarboxamides with glycine derivatives and peptides. *J. Am. Chem. Soc.* **146**, 6307–6316 (2024).
52. Liu, L. et al. Copper-catalyzed intermolecular enantioselective radical oxidative C(sp3)–H/C(sp)–H cross-coupling with rationally designed oxazoline-derived N,N,P(O)-ligands. *Angew. Chem. Int. Ed.* **60**, 26710–26717 (2021).
53. Wang, C.-Y. et al. Enantioselective copper-catalyzed remote C(sp^3)–H alkynylation of linear primary sulfonamides. *Org. Lett.* **22**, 4006–4009 (2020).
54. Zhang, Z.-H. et al. Copper-catalyzed enantioselective Sonogashira-type oxidative cross-coupling of unactivated C(sp3)–H bonds with alkynes. *Nat. Commun.* **10**, 5689 (2019).
55. Chen, H., Jin, W. & Yu, S. Enantioselective remote C(sp^3)–H cyanation *via* dual photoredox and copper catalysis. *Org. Lett.* **22**, 5910–5914 (2020).
56. Liu, R.-Z. et al. Generation and reactivity of amidyl radicals: manganese-mediated atom-transfer reaction. *Angew. Chem. Int. Ed.* **59**, 4428–4433 (2020).
57. Qin, Q. & Yu, S. Visible-light-promoted remote C(sp^3)–H amidation and chlorination. *Org. Lett.* **17**, 1894–1897 (2015).
58. Zeng, X. et al. Copper-catalyzed, chloroamide-directed benzylic C–H difluoromethylation. *J. Am. Chem. Soc.* **141**, 19941–19949 (2019).
59. Fan, W. et al. Electrophotocatalytic decoupled radical relay enables highly efficient and enantioselective benzylic C–H functionalization. *J. Am. Chem. Soc.* **144**, 21674–21682 (2022).
60. Yusan, B., Amuti, A., Xu, X. J. & Wusiman, A. NIS/TEMPO-promoted oxidative cyanation and nitro-mannich reaction of tertiary amines. *Eur. J. Org. Chem.* **27**, e202400144 (2024).
61. Grundke, C. et al. Photochemical α-aminonitrile synthesis using Zn-phthalocyanines as near-infrared photocatalysts. *J. Org. Chem.* **87**, 5630–5642 (2022).
62. Xu, F. et al. Iron(III)-catalyzed α-cyanation and carbonylation with 2-pyridylacetonitrile: divergent synthesis of α-amino nitriles and tetrahydroisoquinolinones. *Org. Biomol. Chem.* **20**, 7031–7035 (2022).
63. Lennox, A. J. J. et al. Electrochemical aminoxyl-mediated α-cyanation of secondary piperidines for pharmaceutical building block diversification. *J. Am. Chem. Soc.* **140**, 11227–11231 (2018).
64. Suzuki, K., Tang, F., Kikukawa, Y., Yamaguchi, K. & Mizuno, N. Visible-light-induced photoredox catalysis with a tetracerium-containing silicotungstate. *Angew. Chem. Int. Ed.* **53**, 5356–5360 (2014).
65. Yamaguchi, K., Wang, Y. & Mizuno, N. A widely applicable regioselective aerobic α-cyanation of tertiary amines heterogeneously catalyzed by manganese oxides. *ChemCatChem* **5**, 2835–2838 (2013).
66. Wang, F.-L. et al. Mechanism-based ligand design for copper-catalysed enantioconvergent C(sp^3)–C(sp) cross-coupling of tertiary electrophiles with alkynes. *Nat. Chem.* **14**, 949–957 (2022).
67. Shimizu, D., Kurose, A. & Nishikata, T. Remote nucleophilic substitution at a C(sp^3)–H bond of α-bromocarboxamides *via* 1,4-hydrogen atom transfer to access *N*-acyl-*N*,*O*-acetal compounds. *Org. Lett.* **24**, 7873–7877 (2022).
68. Xie, J. et al. New catalytic radical process involving 1,4-hydrogen atom abstraction: asymmetric construction of cyclobutanones. *J. Am. Chem. Soc.* **143**, 11670–11678 (2021).
69. Simmons, E. M. & Hartwig, J. F. On the interpretation of deuterium kinetic isotope effects in C–H bond functionalizations by transition-metal complexes. *Angew. Chem. Int. Ed.* **51**, 3066–3072 (2012).
70. Chen, X. et al. Mechanistic insights into copper-mediated benzylic C(sp^3)–H bond trifluoromethylation. *Org. Biomol. Chem.* **22**, 8480–8487 (2024).
71. Fang, C. et al. Mechanistically guided predictive models for ligand and initiator effects in copper-catalyzed atom transfer radical polymerization (Cu-ATRP). *J. Am. Chem. Soc.* **141**, 7486–7497 (2019).

Acknowledgements

This work was supported by National Natural Science Foundation of China (No. 22301275 for Y.-J.M., 22371256 for Y.-F.Y.), the Research

Foundation for Advanced Talents from ZJUT (No. 2021101016929 for S.-J.L.), Zhejiang Provincial Natural Science Foundation of China (LMS25B020004 for S.-J.L., LR25B020002 for Y.-F.Y.), Beidou Scientific Research Project of Zhejiang University of Technology (D.-Q.X.), and the Fundamental Research Funds for the Provincial Universities of Zhejiang (RF-C2022006 for Y.-F.Y.).

Author contributions

S.-J.L., D.-Q.X., and Z.-Y.X. conceived and designed the project. Y.-J.M. developed the reaction and prepared the supplementary information. Y.-F.Y. and X.C. designed and performed the DFT calculations. Q.P., H.-L.L., and K.Z. performed the experiments and collected the data. Y.-J.M. and S.-J.L. prepared the manuscript with feedback from all co-authors.

Competing interests

The authors declare no competing interests.

Additional information

Supplementary information The online version contains supplementary material available at https://doi.org/10.1038/s41467-026-68598-8.

Correspondence and requests for materials should be addressed to Yun-Fang Yang, Shao-Jie Lou or Dan-Qian Xu.

Peer review information *Nature Communications* thanks Shuichi Nakamura and the other anonymous reviewer(s) for their contribution to the peer review of this work. A peer review file is available.